Published in final edited form as:
*Dev Biol*. 2011 November 1; 359(1): 59–72. doi:10.1016/j.ydbio.2011.08.011.

# The FGD Homologue EXC-5 Regulates Apical Trafficking in *C. elegans* Tubules

**Brendan C. Mattingly** and **Matthew Buechner**
Dept. of Molecular Biosciences, University of Kansas, Lawrence, KS, 66045

## Abstract

Maintenance of the shape of biological tubules is critical for development and physiology of metazoan organisms. Loss of function of the *C. elegans* FGD protein EXC-5 allows large fluid-filled cysts to form in the lumen of the single-cell excretory canal tubules, while overexpression of *exc-5* causes defects at the tubule's basolateral surface. We have examined the effects of altering expression levels of *exc-5* on the distribution of fluorescently-marked subcellular organelles. In *exc-5* mutants, early endosomes build up in the cell, especially in areas close to cysts, while recycling endosomes are depleted. Endosome morphology changes prior to cyst formation. Conversely, when *exc-5* is overexpressed, recycling endosomes are enriched. Since FGD proteins activate the small GTPases CDC42 and Rac, these results support the hypothesis that EXC-5 acts through small GTPases to move material from apical early endosomes to recycling endosomes, and that loss of such movement is likely the cause of tubule deformation both in nematodes and in tissues affected by FGD dysfunction such as Charcot-Marie-Tooth Syndrome type 4H.

### Keywords

Charcot-Marie-Tooth Syndrome; FGD; EEA1; RME-1; Rab; CDC42; endosome recycling

## Introduction

The formation and maintenance of epithelial tubule structure is essential for organogenesis in all metazoan organisms. Formation of such tubules requires apical polarization to create the luminal and basolateral membranes, followed by secretion of material to create the internal lumen (Lubarsky and Krasnow, 2003). Once formed, it is critical that the lumen diameter be maintained in order to allow proper transport of material (Harris and Torres, 2008). Recent studies have investigated the formation of the tubular apical surface in cell culture (Martin-Belmonte and Mostov, 2008; Rodriguez-Fraticelli et al., 2010) and in models such as the *Drosophila* trachea (Levi et al., 2006; Luschnig et al., 2006) and mammalian tissues (Kesavan et al., 2009; McCaffrey and Macara, 2009), but less is known about how such structures maintain their diameter once the tubule is formed.

The excretory canal cell of the nematode *C. elegans* is a single-celled epithelium that forms tubules to regulate organismal osmolarity and ionic content (Hahn-Windgassen and Van



**Corresponding Author:** Matthew Buechner, Dept. of Molecular Biosciences, 1200 Sunnyside Drive, 8035 Haworth Hall, University of Kansas, Lawrence, KS, 66045-7534, buechner@ku.edu (785) 864-4328 FAX: (785) 864-5294.

Gilst, 2009; Nelson and Riddle, 1984; Teramoto et al., 2010). During the second-half of embryogenesis, this cell forms long fluid-filled tubules called canals that continue to extend throughout the first larval stage (Buechner et al., 1999) (Fig. 1A, B). Extension of these tubules along the length of the entire organism requires simultaneous creation of basolateral surface along the outside of the tubule together with apical surface on the luminal side. Once initial formation of the canals is complete, the material of the two surfaces must further be recycled so as to alter tubule length and diameter as the animal enlarges through four larval stages and adulthood, and to repair any damage that occurs to the tubules through body-bending movement.

Mutations of any of a series of *exc* genes cause the canals' apical cytoskeleton to fail, which allows the lumen to expand into fluid-filled cysts (Buechner, 2002). The cloned canal-expressed *exc* mutants encode ion channels and their regulators (Berry et al., 2003; Hisamoto et al., 2008; Liegeois et al., 2007), cytoskeletal proteins (Gao et al., 2001; Gobel et al., 2004; Praitis et al., 2005; Suzuki et al., 2001; Tong and Buechner, 2008), and an RNA-transport protein (Fujita et al., 2003). Loss-of-function mutations of *exc-5* causes defects in the apical (luminal) surface of the excretory canals by allowing formation of large cysts predominantly at the growing tips of excretory canals (Fig. 1C), while overexpression of *exc-5* causes failure of the basolateral surface of the cell, so that the normal-diameter luminal surface is convoluted inside a cell body that fails to extend (Fig. 1D) (Suzuki et al., 2001). *exc-5* encodes a homologue of the FGD family of mammalian guanine exchange factors (Suzuki et al., 2001, Mattingly, 2011). Mutation of human FGD genes cause Faciogenital Dysplasia (FGD1) (Pasteris et al., 1994), and Charcot-Marie-Tooth disease type 4H (FGD4) (Delague et al., 2007). The human EXC-5 homologue FGD1 activates the small Rho-GTPase CDC42 when overexpressed in 3T3 fibroblasts in tissue culture (Olson et al., 1996). CDC-42 has multiple roles in transport of vesicles in synthesis and recycling in epithelial cells (reviewed in (Harris and Tepass, 2010)), and can mediate differential transport of vesicles at the apical vs. the basolateral surfaces (Harris and Tepass, 2008; Rojas et al., 2001).

In order to understand the subcellular processes that underlie the cystic and convoluted tubule phenotypes we observe when dosage of *exc-5* is perturbed, we created a set of excretory canal markers to label various subcellular compartments. We found that within the excretory canals, the number and distribution of several of the compartments depended heavily on normal levels of EXC-5. The most strongly affected compartments, early endosomes and recycling endosomes, recycle cellular components. In addition, expression of a fragment of WSP-1 that binds to activated CDC-42 caused similar effects on canal structure as did expression of EXC-5. These results support the hypothesis that EXC-5 and other FGD proteins modulate small GTPase activity to move material from early endosomes to recycling endosomes, and this movement maintains the structure of the apical surface of these epithelia.

## Materials and Methods

### Nematode Genetics

*C. elegans* mutants were derived from the N2 Bristol strain background. All strains were grown on *E. coli* strain BK16 (a Streptomycin-resistant derivative of OP50) and maintained as described (Brenner, 1974).

## DNA Constructs

The *exc-5::gfp* construct was a gift from K. Matsumoto. It contains 12.6kb of genomic DNA comprised of 7.2kb of upstream sequence from *exc-5* and 5.3kb of *exc-5* coding region placed into pPD95.75 (gift from A. Fire) in front of the *gfp* gene and an *unc-54* 3′ UTR.

Plasmid pCV01 is the generous gift of T. Oka and M. Futai, and contains the promoter for *vha-1* in front of *gfp* (Oka et al., 2001); this construct is strongly expressed in the excretory canal cell and head mesodermal cell. Nematode lines BK30 and BK36 contain a stable integration (*qpIs11*) of pCVO1 together with the *unc-119* gene, transformed into *unc-119* animals that were either wild-type (BK36) or *exc-5*(*rh232*) (BK36) for canal morphology, via biolistic transformation by the method of (Praitis et al., 2001). Each integrant was outcrossed at least 5 times. For BK36, the site of integration was mapped to LG I.

Plasmids containing constructs expressing constitutively active (ca, G12V) and dominant-negative (dn, T17N) forms of nematode *cdc-42* linked to the marker *gfp* were the gift of E. Lundquist. A 1.2 kb NheI genomic fragment was amplified and recloned into pPD117.01 (created by A. Fire, gift of L. Timmons) by use of standard molecular techniques.

Subcellular marker Gateway® (Invitrogen Corporation) constructs were a generous gift from B. Grant. The *vit-2* promoter in the mCherry expression vector was excised as a 326bp SphI-KpnI fragment and replaced with a 1.4kb *exc-9* promoter by use of standard molecular techniques. The modified vector was then used in a series of nine Gateway® reactions with each of the donor vectors containing either the cDNA of nematode *rab-5, rab-7, rab-11, glo-1*, or *rme-1* (splice form d); or genomic copy of nematode *cdc-42, eea-1*, or *chc-1* genes; or the GRIP (Glutamate Receptor-Interacting Protein) domain of nematode gene T05G5.9 (gift of B. Grant and S. Eimer). The result of each reaction was the *exc-9*-promoted *mCherry* cDNA fused N-terminally to the specific subcellular gene.

The G-protein-binding domain (GBD) of *wsp-1* (Kumfer et al., 2010) was PCR-amplified from constructs generously provided by Jayne Squirrel, Kraig Kumfer, and John White, and then cloned into a pENTR™/D-TOPO® vector (Invitrogen Corporation). This sub-clone was used as above to create *mCherry* cDNA fused N-terminally to *GBDwsp-1* expressed via the *exc-9* promoter.

## Microinjection and Integration of Constructs

Subcellular constructs were injected into the rachis of young adult N2 animals at a concentration of 50 and 100ng/μl. Transgenic $F_1$ animals were isolated to separate plates and screened for array transmission.

A stable low-copy-number array of *exc-5::gfp* driven by the *exc-5* promoter was obtained via microinjection of the $P_{exc\text{-}5}$*::exc-5::gfp* construct at 15ng/μl mixed with 25ng/μl of N2 genomic DNA. Array transmission in this strain was 0.6% (n=300). Unstable low-copy transient arrays of altered *cdc-42* forms driven by the *vha-1* promoter were obtained via microinjection of the *Pvha-1::gfp::cdc-42* (dn or ca) construct at 10ng/μl.

Stable arrays were integrated into the nematode chromosome through the use of 4,5′,8-trimethylpsoralen (TMP) (Yandell et al., 1994). Nematodes were washed off plates with M9 buffer, pelleted, and resuspended in a minimal volume. TMP was added to a final concentration of 30μg/ml. Animals were soaked in the TMP solution for 15 minutes in the dark and washed twice in M9 buffer. Nematodes were then plated and irradiated by use of a Spectrolinker™ (Spectronics Corporation, New York) set to 350μJ at 360nm. $F_2$ progeny from the irradiated animals were isolated and screened for integrants. Plates containing all

fluorescent transgenic progeny were identified as having the transgene homozygously integrated. All integrants were then outcrossed at least five times before use.

### Microscopy

Nematodes were observed via a Zeiss Axioskop microscope with Nomarski optics and epifluorescence using 40x and 63x oil-immersion objectives. Animals were placed on 5% agarose pads in water or PBS containing 0.8% 1-phenoxy-2-propanol as anaesthetic. All images were taken with an Optronics MagnaFire Camera. Images were cropped and merged using the programs GIMP and Graphic Converter (Lemke Software, Peine, Germany).

Time-lapse images were taken by use of the same equipment, except that animals were anaesthetized with 10mM muscimol. Animals were kept at 20°C prior to microscopic observation. Coverslips were sealed with mineral oil to prevent desiccation of the animals.

Confocal images were taken with an Olympus Fluoview FV1000 laser-scanning confocal microscope with 60x objective. Animals were anaesthetized with 10mM muscimol and treated as above.

### Canal Measurements

Posterior excretory canal length was measured relative to the animal length as described (Tong and Buechner, 2008). Animals were kept at 20°C and generally scored as L4 larvae. Canals that did not extend at all or remained near the cell body were scored as (0). Posterior canals that extended to between the cell body and the vulva were scored as (1), at the vulva (2), between the vulva and the tail (3), and full-length canals were scored as a (4). Cysts were counted and grouped according to size. Cysts with a diameter of over half the body width were labeled as large cysts; cysts larger than a quarter of the body diameter up to half the diameter were labeled as medium; cysts a quarter of the body diameter or smaller were labeled as small cysts. A canal that exhibited a lumen that traversed itself more than once was counted as a convoluted tubule.

Relative brightness of markers in cysts vs. noncystic tubules was measured by use of the program NIH ImageJ. Micrographs showing the most anterior cyst of a posterior canal were used, and where possible, micrographs presenting a cyst not adjacent to other cysts were used, since two or more closely spaced cysts concentrated cytoplasm more than did a single cyst. A segmented line of width equal to the widest cyst to be measured was placed over the entire length of the canal, and plot profile was recorded. The average value of the plot profile of the same width of a dark section of the micrograph was subtracted as background. A section of normal-width canal (that did not overlap out-of-focus fluorescence from other tissues or the opposite-side canal) was normalized to relative brightness = 100. The brightest reading of cytoplasm at the junction of cyst and noncystic canals was recorded as “peak brightness,” while the lowest fluorescence along the center of the cyst was recorded as “trough brightness.”

## Results

### EXC-5 dosage at the apical surface determines canal morphology

Previous work has shown that null mutation of *exc-5* in the excretory canal results in the formation of large fluid-filled cysts along the length of and especially at the distal tips of the canal (Fig. 1C), while strong overexpression of *exc-5* in the canal causes a “convoluted tubule” phenotype in which the apical surface and cytoskeleton maintain the correct diameter, but are wrapped inside a large cell body that fails to extend processes along the hypoderm (Fig. 1D) (Suzuki et al., 2001). We found that microinjection of higher

concentrations (>50 ng/μl) of an *exc-5*::*gfp* construct resulted in dead eggs and larvae that died at the L1 or L2 stage. Microinjection of varying concentrations of the *exc-5*::*gfp* construct at lower levels (5-25 ng/μl) resulted in progeny exhibiting tubule convolutions of severity proportionate to concentration of DNA injected (Fig. 1D). In order to examine the subcellular location of EXC-5 within the canal, we integrated a stable low-copy-number *exc-5*::*gfp* transgene into the chromosome (integrant *qpIs78*). This integrated construct, present as a heterozygote, fluoresces very weakly (barely visible in a compound fluorescence microscope), and rescues the null mutant Exc-5 phenotype to create near-normal-length canals that each contain a normal-diameter lumen (data not shown). Since the null mutant Exc-5 phenotype is fully recessive, our results are consistent with the transgene expressing approximately a single dose of EXC-5 protein. The *exc-5*::*gfp* transgene was also expressed in other tissues previously reported to contain this protein, including the pharynx (Suzuki et al., 2001); confocal microscopy showed the protein appearing along actin fibers in the pharyngeal muscles (Fig. 1E).

Diploid wild-type N2 animals have 2 copies of *exc-5*, so when the *exc-5* transgene is present heterozygously in N2 canals, the total dosage of *exc-5* is (presumably) 3 copies, and the animals exhibit a normal canal phenotype. When the transgene is present homozygously (strain BK179), the total dosage of *exc-5* is increased to 4 copies, and the canals are slightly shortened, and occasionally (8%) form highly convoluted tubules (Table 2). In addition, the diameter of the apical surface was occasionally irregular, with constricted areas (Fig. 1F). Examination at high magnification confirmed previous results demonstrating that the EXC-5 protein is located both in the cell body and throughout the length of the canal. The apical surface of the canal extends into the cell cytoplasm through a network of small vesicular tubules called canaliculi (Nelson et al., 1983), so that apical EXC-5 generally appears as a thick layer surrounding the lumen when viewed via light microscopy. Nevertheless, we found that EXC-5 is enriched on the apical (luminal) side of the cytoplasm, but beneath the surface of the tubule lumen (Fig. 1G-I). Apical clathrin (CHC-1) appears enriched in the same area of high concentration of EXC-5, which may indicate that clathrin-coated pits and EXC-5 are both found in the region of myriad tubulovesicular canaliculi that extend into the cytoplasm from the apical surface (Nelson et al., 1983). Canal structure appears to provide a sensitive reflection of EXC-5 dosage, with the degree of shortening and convolution indicating higher levels of EXC-5 dosage at the apical surface.

## Subcellular Organelles Appear Throughout the Entire Length of the Excretory Canals

In *exc-5* mutants the canals initially form normally, but then develop large cysts predominantly at the growing tips of the tubules (Buechner et al., 1999). Since the majority of lumen initially forms with a normal diameter, it is likely that the defect in these mutants involves the continual reformation of components directed to maintain apical structure as the animal grows and moves, rather than the initial placement of cytoskeleton. During recycling, membrane-bound proteins are taken up either via clathrin-coated pits or via clathrin-independent pathways (Grant and Donaldson, 2009) (Fig. 2A). The material is transported via endocytic vesicles into early endosomes, where the material is either shuttled via late endosomes to lysosomes to be destroyed, or brought back to the surface by way of recycling endosomes. We examined the location of multiple components of the recycling machinery within the excretory canals by adapting a set of eight constructs expressing marker proteins specific to different subcellular organelles linked to the fluorescent tag mCherry for canal expression. We also made similar markers for the putative EXC-5 substrate protein CDC-42 (constructs generously provided by B. Grant) as well as the G-protein-binding domain of the WASP homologue WSP-1 that binds to activated CDC-42 (graciously provided by J. White, K. Kumfer, and J. Squirrell) (Kumfer et al., 2010), and transiently expressed constitutively-active (T17N) or dominant-negative (G12V) forms of CDC-42 (constructs generously

provided by E. Lundquist). Stably integrated markers were expressed through the *exc-9* promoter in the excretory canal starting at the 3-fold stage, as well as in the uterine seam cell and several neurons (Tong and Buechner, 2008). The *exc-5* promoter was not used, in order to avoid the possibility that expression of the construct would deplete transcription factors specific to *exc-5* in the canal, and thereby decrease expression of EXC-5 in the cell. Under control of the *exc-9* promoter, some of the constructs did cause minor defects in canal morphology in a wild-type background (Fig. 2B-F) (Table 2). Expression of the wild-type form of the small GTPase CDC-42 linked to mCherry caused 21% of the animals to develop very small cysts near the distal tips of the canals. Expression of mCherry-linked WSP-1-GBD, which binds to GTP-bound CDC-42, greatly shortened the canals, with a widened (though only occasionally cystic) lumen diameter towards the distal end of the lumen, sometimes followed by a "tail" of cytoplasm containing no lumen (Fig. 2D). Transient expression of constitutively-active or wild-type CDC-42 or also caused formation of cytoplasmic "tails," while causing convolutions similar to those seen in animals overexpressing EXC-5 (Table 2). In contrast, the dominant-negative form of CDC-42 caused formation of cysts throughout the canal in a majority of animals examined (Table 2), although the cysts were not quite as large or as frequent as in mutants of *exc-5*. These results are consistent with EXC-5 functioning at least in part through the activation of CDC-42.

Expression of markers labeling specific subcellular organelles had relatively smaller effects on canal morphology (Table 2). In 35% of canals examined, RAB-7 expression caused moderate shortening of the canal with neither cyst nor convoluted tubule formation. Expression of the endocytic vesicle marker RAB-5 had less of a canal-shortening effect (19% moderately affected), and caused a convoluted tubule in 9% of the animals. Finally, expression of the recycling endosome marker RAB-11 on occasion caused small cysts to form (2% of the animals), and also caused a convoluted tubule in 7% of the animals. In the great majority of animals expressing these constructs, however, the sensitive canal morphology was normal, consistent with marker expression not causing substantial changes in subcellular trafficking.

The fluorescence of all 9 marker proteins was highest near the excretory canal cell body, and decreased along the length of the canals (Supp. Fig. 1). This distribution mirrors the placement of endoplasmic reticulum and Golgi bodies, which are also found throughout the canals as well as in the cell body (Buechner et al., 1999; Nelson et al., 1983). Since cysts initially develop toward the tips of *exc-5* mutant animals during late embryogenesis (Buechner et al., 1999), when the posterior canals have extended only halfway towards their full length (Fujita et al., 2003), we examined marker location primarily anterior to the vulva in order to compare the distribution of subcellular components in wild type and in cystic mutants. The canals are also wider closer to the excretory cell body (Chitwood and Chitwood, 1974; Nelson et al., 1983), which facilitates determination of the apical/basal placement of vesicles in the canals.

The marker for clathrin-coated pits, CHC-1 (clathrin heavy chain), was located in a thin uniform layer on both the apical and basolateral surfaces of the canals, with frequent higher concentrations in discrete puncta (Figs. 1G-I, 3A). The bulk of EXC-5 fluorescence did not overlap with the location of CHC-1.

Early endosomes, as marked by RAB-5 (Chavrier et al., 1990) and by EEA-1 (Mu et al., 1995), are distributed irregularly along the length of the canal (Fig. 3B, C). Occasional larger accumulations of EEA-1 were observed near the cell body at both the basal and apical surfaces of the canal.

Lysosomes and late endosomes were found in puncta spaced irregularly along the length of the canals (Fig. 3D, E). Late endosomes were marked with a RAB-7 (Chavrier et al., 1990) marker, while the marker GLO-1/Rab38 was used to detect lysosomes (Hermann et al., 2005).

Recycling endosomes were marked by RAB-11 and RME-1 (Fig. 3F, G). RAB-11 displayed mainly diffuse staining throughout the cell, with a few puncta irregularly placed along the canals. RME-1-marked vesicles were generally larger and far more numerous than were puncta labeled by RAB-11. In both cases, the number of puncta was highest near the cell body, but puncta were evident throughout the entire length of the canals.

Golgi bodies, marked by a Golgi-targeting GRIP domain (Kjer-Nielsen et al., 1999; Munro and Nichols, 1999) were also seen throughout the canals, though most prominently near the cell bodies (Fig. 3H). GRIP fluorescence appeared punctate throughout the distal canals. Finally, CDC-42, the presumptive target of EXC-5, was located diffusely throughout the cytoplasm of the excretory canals, with highest fluorescence levels towards the apical surface of the canals. Expression of GBD-WSP-1 linked to mCherry, marking activated CDC-42, showed diffuse fluorescence throughout the cytoplasm similar to that of CDC-42 (Fig. 3I), but in addition appeared as occasional puncta throughout the canal (Fig. 3J).

All of the markers were evident throughout the length of both growing and adult full-grown canals, which suggests that material throughout the canals is steadily and continually being taken up from canal surfaces and recycled, while material from the Golgi bodies can be transported to the canals.

## Loss of EXC-5 Activity Disrupts Endosome Morphology

In order to determine if EXC-5 mediates endocytic trafficking, as has been found for CDC-42 (Rojas et al., 2001), the subcellular marker expression constructs were crossed into the *exc-5*(*rh232*) null allele strain. Cyst formation caused canal cytoplasm to accumulate at the point where the tubule widened, and between adjoining cysts, as seen via a cytoplasmic GFP marker (Fig. 4A). The distribution of labeled CHC-1, CDC-42, GBD-WSP-1, RAB-7, GLO-1, RAB-11, and GRIP was generally unaffected by loss of EXC-5 activity, as compared to the cytoplasmic GFP controls (Supp. Fig. 2) (Table 3). The placement, approximate number, and distribution of puncta in these mutants appeared quite similar to their appearance in wild-type animals, with similar amounts of marked clathrin-coated pits, late endosomes, and lysosomes.

Loss of EXC-5 activity often caused a strong effect on the distribution of EEA-1 and RME-1 markers, as well as some infrequent but large effects on RAB-5 distribution (Table 3, Fig. 4). Early endosome marker EEA-1 was no longer seen in discrete puncta, but rather accumulated into large irregular shapes. These accumulations were often evident in the areas of the canals immediately adjacent to and surrounding the large cysts. In 58% of canals, the accumulation of labeled EEA-1 surrounding the cysts appeared substantially brighter than in the normal-diameter tubule anterior to the cyst. Labeled RAB-5 (marking early endosomes) was also sometimes (24%) enriched near cysts in *rh232* animals, but while these accumulations were much brighter than for some markers, the frequency of RAB-5 accumulations was similar to that of cytoplasm surrounding the cysts. Most strikingly, in 31% of animals, labeled RME-1 was the only marker to exhibit a strong and opposite phenotype: Other than near the excretory cell body, the amount of labeled RME-1 was severely depleted throughout the canals, and almost entirely absent in the cytoplasm surrounding large cysts. Taken together, these results suggest a defect in recycling endosome transport in *exc-5* mutants.

### Overexpressed EXC-5 Affects Recycling Endosomes

The subcellular markers were also crossed into strains containing the integrated *exc-5*::*gfp* construct (at a presumed expression level of ~4 copies of functional EXC-5). Overexpression of EXC-5 also showed little effect on most of the subcellular markers (Supp. Fig. 3), but showed strong interactions with RME-1 and EEA-1 (Figs. 4, 5). Overexpression of *exc-5* together with the *rme-1* marker caused higher than normal accumulation of mCherry::RME-1 puncta, whereas the level of labeled EXC-5 became depleted (Figs. 4D, 5A), consistent with a model in which EXC-5 ferried excess amounts of material from early endosomes to recycling endosomes. The effect of *exc-5* overexpression was even more striking when combined with the *mCherry*::*eea-1* marker (Figs. 4B, 5B-D). Expression of homozygous *mCherry*::*eea-1* was lethal in the homozygous *exc-5*::*gfp* strain; animals died during late embryogenesis, though no effects on canal morphology were obvious (Fig. 5C, D). Heterozygous expression of the *mCherry*::*eea-1* construct in animals homozygous for the *exc-5*::*gfp*-integrated transgene (with milder overexpression) allowed animals to survive, and showed somewhat fewer, but larger, puncta of mCherry::EEA-1 along the apical surface (Fig. 5B). Both loss and overexpression of EXC-5 activity therefore perturbed EEA-1- and RME-1-marked endosomes.

### EXC-5 Shows Genetic Interactions with the Rho GTPase CDC-42

The human EXC-5 homologue FGD1 activates the small Rho-GTPase CDC42 when overexpressed in 3T3 fibroblasts in tissue culture (Olson et al., 1996). As noted above, in *C. elegans*, overexpression of *mCherry*::*cdc-42* increased the formation of small cysts along the length of shortened canals in wild-type, *exc-5* mutant, and *exc-5*-overexpressing animals (Table 2). Expression of *mCherry*::*cdc-42* in animals that overexpressed EXC-5 resulted in substantially shorter, more convoluted tubules. In those convoluted excretory cells, fluorescent CDC-42 is found throughout the cell, but is strongest in the regions surrounding the convoluted lumens, where the canaliculi associated with tubules are located. (Fig. 6A). Fluorescent EXC-5 is located almost exclusively in this same region, and is noticeably greatly enriched just adjacent to the tubule lumen (Fig. 6B, C), which is enriched with dense filaments (Buechner et al., 1999). These results are consistent with the evidence from Table 2 that EXC-5 acts at least in part through activation of CDC-42.

### Accumulation of Early Endosomes Precedes Cyst Formation

To test whether the accumulation of early endosomal material adjacent to cysts was the cause or a result of cyst formation, we examined the location of early endosomal markers EEA-1 and RME-1 in *rh232* animals prior to and during the formation of excretory canal cysts (Fig. 7). Cysts initially formed in the late stages of embryogenesis and early first larval stage. Cysts formed suddenly and were initially small in size. In *exc-5* mutants, these cysts formed at the end of both anterior and posterior canals, but occasionally developed in additional isolated areas along the length of the canal.

The EEA-1 marker showed altered location during the process of cyst formation. In animals containing only the *mCherry*::*eea-1* integrant, there was little visible EEA-1 accumulation along the length of the canal even after the animal hatched (Fig. 3C). When expressed in *rh232* animals, however, there appeared strong build-ups of mCherry::EEA-1 during embryogenesis in regions of the canal prior to cyst formation (Fig. 7). Continuous observation of these canals showed the rapid development of cysts at the locations where EEA-1::mCherry had accumulated. Observation of the embryonic canals is difficult, since lumen diameter is at the resolution limit of light microscopy and the animals move rapidly during late embryogenesis. Nevertheless, four embryos were able to be observed closely, with accumulations of EEA-1 becoming visible in the canals prior to formation of cysts in those spots in all cases. Since accumulation of EEA-1 precedes the appearance of cysts, we

conclude that disruption of EXC-5-mediated endosome regulation in *exc-5* mutants precedes and is therefore likely the cause of failure of the structural support of the apical surface that allows collapse of the tubule into fluid-filled cysts.

## Discussion

### EXC-5 mediates movement of material from apical early endosomes to recycling endosomes

All cells must constantly recycle and move material in order to accommodate growth and movement of the animal. Membrane curvature is most acute in narrow tubules, and cannot be easily maintained without maintenance of proteins to support that curvature (Graham and Kozlov, 2010). Osmotic pressure constantly exerts force to expand the tubule. Nematodes continuously bend back and forth, additionally stressing the narrow excretory canals. In the excretory canals, loss of proteins such as integrin, intermediate filament A2, or Unc-53 (neuron navigator) at the basolateral surface cause misdirection and shortening of tubule outgrowth, but does not affect lumen diameter (Hedgecock et al., 1987, Shioi et al., 2001, Stringham and Schmidt 2009). We hypothesize that failure of the structural support of the apical surface allows osmotic pressure to form fluid-filled cysts rapidly. EXC proteins thus prevent loss or weakening of the apical canal surface (Buechner et al., 1999). As seen here and in previous work, overexpression of EXC-5, EXC-9, or constitutively-active CDC-42 proteins allow the tubule to form and maintain a normal diameter, but prevents extension of the canals along the basal surface, which results in a convoluted tubule (Suzuki et al., 2001; Tong and Buechner, 2008). Similar results have been seen in *C. elegans* mosaic animals deficient in basolateral or basement membrane proteins (integrin, laminin) (Gettner et al., 1995; Hedgecock et al., 1987), as well as in the narrow single-celled tubular termini of *Drosophila* trachea deficient in talin or integrin (Levi et al., 2006). We infer that EXC proteins that mediate intracellular trafficking primarily exert their effects on movement of vesicles to or from the apical surface, but that overexpression of these proteins can prevent normal basolateral trafficking as well.

Uptake of material via the clathrin-coated pits places material into early endosomes, where it is either sorted to be destroyed in lysosomes, or returned through recycling endosomes back to the cell surface (Grant and Donaldson, 2009). Expression of multiple labeled markers for subcellular compartments found that all of these compartments are at greatest concentration near the excretory cell body, but are all present throughout the length of the canals. These results confirm previous electron micrographic studies that showed endoplasmic reticulum, Golgi, multivesicular bodies, lysosomes, and a myriad of tubulovesicular structures throughout the excretory canals, especially near the apical (luminal) surface (Buechner et al., 1999; Nelson et al., 1983).

The results presented here show that the EXC-5 guanine exchange factor plays a critical role in regulating endosome morphology and probably function at the apical surface in the canals. When *exc-5* is deleted, most of the mCherry-labeled markers retained the position and intensity observed in wild-type animals, with the exception of labeled EEA-1, RAB-5, and RME-1. Without EXC-5 present, RME-1/EHD, found on labeled recycling endosomes (Grant and Donaldson, 2009; Naslavsky and Caplan, 2005), appeared gradually depleted, while RAB-5 and EEA-1, markers for early endosomes, abnormally accumulated. The EEA-1 marker in particular formed large irregular accretions especially surrounding cysts. Such enlarged endosomes are a hallmark of blocked recycling (Chen et al., 2006; Sharma et al., 2008). Most strikingly, progressive studies showed that the accumulations of EEA-1 formed at these locations prior to the formation of cysts, and could in fact be used to predict the sites of cyst formation. We infer that EXC-5 is needed for the movement from apical early endosomes to recycling endosomes. In this model (Fig. 8), when EXC-5 is missing,

apical surface proteins that guide reformation and strengthening of the cytoskeleton are taken up into endocytic vesicles, but cannot pass further into recycling endosomes to be returned to the surface, so that the apical cytoskeleton is thinned and weakened, ultimately to collapse (Fig. 8B). When *exc-5* is overexpressed, the apical surface is maintained; we hypothesize that so much trafficking occurs at the apical surface that traffic from the basal surface is slowly winnowed, leading to inability of the canal to extend properly, so that the cell forms convoluted tubules of normal diameter inside an enlarged cell body (Fig. 8C). Such a balance of apical to basal endocytic trafficking mediated by Rho proteins such as Cdc42 has been found to be important for the maintenance of polarity in mammalian epithelial cells (Rojas et al., 2001; Rondanino et al., 2007), and similar defects in subcellular trafficking were previously reported in *C. elegans* coelomocytes upon depletion of CDC-42 via RNAi (Balklava et al., 2007).

### The Excretory Canals Are a Sensitive Indicator of Endosomal Movement and Structure

The labeled markers used here have previously been found to label distinct structures in nematode intestinal cells and coelomocytes (Grant and Donaldson, 2009; Pant et al., 2009; Shi et al., 2007). Although the distance from apical to basal surface is much smaller in the canals vs. wide intestinal cells, the markers labeled distinct locations within the canals. In addition, the great length of the canals (the longest cell in the organism) provides an exquisitely sensitive indicator of the effects of trafficking on cell structure. The distance from nucleus to distal cell surfaces is magnified, so that differences in endosome concentration along the length of the canals are easily apparent. As a result, mild changes in the dose of EXC-5 produced rapid formation of easily detectable cysts, or of convolutions in the path of the canals.

Expression of a few of the markers by themselves occasionally showed effects on canal structure. In rare cases, this expression caused the tip of the apical surface to come loose from the tip of the basal surface, which resulted in formation of a narrow “tail” of cytoplasm without a lumen (Fig. 2D). Expression of marked RAB-5 or RAB-11 caused the canals at low but significant penetrance (7-9%, Table 2) to exhibit the strongly convoluted canal structure caused by overexpression of functional EXC-5 or EXC-9 (Tong and Buechner, 2008), in which the apical tubule is maintained at its proper diameter and length, but the basal surface fails to extend. One possible explanation is that overexpression of any of these proteins increases the rate of turnover of endosomes from the apical surface, which then monopolizes the recycling pathways such that membrane proteins from the basal surface are not efficiently recycled. Overexpression of RAB proteins can alter the ratio of endosome movement via different pathways; e.g. in mammalian cells, RAB-11 overexpression forced material away from movement into lysosomes towards greater amounts of recycling (Moore et al., 2004; Ren et al., 1998). Expression of constitutively activated RAB-5 causes the formation of enlarged endosomes (Bucci et al., 1992; Stenmark et al., 1994), but that effect was not seen here in canals with wild-type levels of EXC-5. In canals overexpressing EXC-5, expression of labeled EEA-1 did cause enlargement of endosomes. It will be interesting to observe the effects on canal structure caused by manipulation of other proteins that regulate trafficking.

### EXC-5 as a Model for FGD Activity

EXC-5 is homologous to the FGD family of four mammalian guanine exchange factors (Gao et al., 2001; Suzuki et al., 2001, Mattingly, 2011). These genes include FGD1, which is defective in Aarskog-Scott Syndrome, a developmental syndrome in which the skeleton of the jaws and limbs are malformed (Pasteris et al., 1994); and FGD4, the locus of Charcot-Marie-Tooth Syndrome Type 4H (CMT4H), a muscular dystrophy (Delague et al., 2007). FGD1 has been shown in 3T3 cells to activate the Rho-GTPase CDC42, but also had other

effects not mediated through CDC42 (Ono et al., 2000; Whitehead et al., 1998). We found similar effects here. Transient expression of constitutively active CDC-42, as well as stable expression of the small GBD-WSP-1 (which binds to activated CDC-42 (Kumfer et al., 2010)), both exerted effects on the canal similar to that of EXC-5 overexpression. Both in wild-type animals and mutants lacking EXC-5 function, expression of WSP-1 GBD caused shortening of the canals and formation of convoluted tubules, similar to the effects of EXC-5 overexpression (Table 2). Transient expression of constitutively active CDC-42 had the same effect in wild-type animals. In addition, when the *exc-5* gene was overexpressed, expression of WSP-1 GBD had little further effect on canal morphology, consistent with EXC-5 overexpression having already activated CDC-42. Finally, transient expression of dominant-negative CDC-42 in wild-type worms caused defects in canal morphology similar to that caused through loss of EXC-5 activity. We infer that EXC-5 and WSP-1 GBD may cause similar effects on CDC-42 by causing an increase in the amount of this GTPase present in the activated, phosphorylated, form. The GEF activity of EXC-5 likely increases the amount of phosphorylated CDC-42, while perhaps WSP-1 GBD may stabilize phosphorylated CDC-42 here and prevent its transition back to the GDP-bound state.

On the other hand, we saw no obvious differences in the location of labeled GBD-WSP-1 in the canals when EXC-5 was present or deleted. GBD-WSP-1 labeled some puncta, but most of the expression of both GBD-WSP-1 and CDC-42 was cytoplasmic, so it is not clear if activated CDC-42 would have been easily evident in these animals. In addition, constitutively-active CDC-42 did not rescue the cystic phenotype in *exc-5* mutants, which suggests that EXC-5 additionally functions through another pathway. EXC-5 does exhibit genetic interactions with MIG-2, a Rac homologue (Suzuki et al., 2001), and with EXC-9, a homologue of the mammalian LIM-domain protein CRIP (Tong and Buechner, 2008). It will be important to determine if these other proteins similarly affect endosome morphology in the excretory canals and other cells where they are expressed.

In patients with CMT4H, the Schwann cells of the peripheral nervous system develop properly to wrap around neurons to form single-celled tubular insulation. Over the course of years, however, tubules in CMT4H patients develop structural defects strikingly similar in morphology to those of the excretory canals in *exc-5*-deficient mutants, with apparently normal tubules juxtaposed next to swollen regions that no longer insulate the nerves (Stendel et al., 2007). While FGD1 is associated with transport from the trans-Golgi network (Egorov et al., 2009), FGD proteins all contain a FYVE domain that associates with phosphatidylinositol 3-phosphate characteristic of early endosomes (Gaullier et al., 1998). Mammalian FGD1 and FGD2 as well as fungal FGD have all been found associated with early endosomes or plasma membrane (Estrada et al., 2001; Huber et al., 2008; Schink and Bolker, 2009). Based on the results presented here, we suggest that, similar to nematode excretory canals in *exc-5* mutants, Schwann cells in CMT4H patients may be blocked in the recycling of material from early endosomes to recycling endosomes, causing a slow degradation of the apical membrane surface to the point where the cells can no longer maintain a tubule in close contact with the neurons.

Several other Charcot-Marie-Tooth syndrome proteins are necessary for proper trafficking in Schwann cells, including myotubularin-related proteins 2 and 13, LITAF, SH3TC2, and CMT4K, (Azzedine et al., 2003; Bolino et al., 2000; Roberts et al., 2010; Senderek et al., 2003; Stendel et al., 2010). The results presented here indicate that the FGD proteins are likely also involved in regulating the movement of endosomes in Schwann cells. They also suggest that the narrow single-celled tubules of the mammalian Schwann cells, like those of the nematode excretory canals, are a difficult cell structure to maintain, and that endosomal traffic must be delicately balanced in order to accommodate the movement and growth of these polarized cells over the lifespan of the individual.

## Supplementary Material

Refer to Web version on PubMed Central for supplementary material.

## Acknowledgments

We are indebted to Drs. Barth Grant, Erik Lundquist, Brian Ackley, Toshihiko Oka, Masamitsu Futai, John White, Kraig Kumfer, Jayne Squirrell, and Andrew Fire for the provision of constructs and vectors; the *Caenorhabditis* Genetics Center for provision of constructs and strains; all the members of the University of Kansas Genetics of Development ("GoD") seminar for helpful discussions, and to Drs. Barth Grant and Monica Driscoll for extremely helpful suggestions for this paper. We are especially grateful to Dr. Brian Ackley for being allowed to use his confocal microscope. We are grateful for the competent assistance of Elinor Brown and Derek Setter. This work has been supported by NIH R03 NS067323, the University of Kansas Inez Jay Fund, and the University of Kansas Graduate Research Fund.

## References

Azzedine H, Bolino A, Taieb T, Birouk N, Di Duca M, Bouhouche A, Benamou S, Mrabet A, Hammadouche T, Chkili T, Gouider R, Ravazzolo R, Brice A, Laporte J, LeGuern E. Mutations in MTMR13, a new pseudophosphatase homologue of MTMR2 and Sbf1, in two families with an autosomal recessive demyelinating form of Charcot-Marie-Tooth disease associated with early-onset glaucoma. Am J Hum Genet. 2003; 72:1141–1153. [PubMed: 12687498]

Balklava Z, Pant S, Fares H, Grant BD. Genome-wide analysis identifies a general requirement for polarity proteins in endocytic traffic. Nat Cell Biol. 2007; 9:1066–1073. [PubMed: 17704769]

Berry KL, Bulow HE, Hall DH, Hobert O. A C. elegans CLIC-like protein required for intracellular tube formation and maintenance. Science. 2003; 302:2134–2137. [PubMed: 14684823]

Bolino A, Muglia M, Conforti FL, LeGuern E, Salih MA, Georgiou DM, Christodoulou K, Hausmanowa-Petrusewicz I, Mandich P, Schenone A, Gambardella A, Bono F, Quattrone A, Devoto M, Monaco AP. Charcot-Marie-Tooth type 4B is caused by mutations in the gene encoding myotubularin-related protein-2. Nat Genet. 2000; 25:17–19. [PubMed: 10802647]

Brenner S. The genetics of Caenorhabditis elegans. Genetics. 1974; 77:71–94. [PubMed: 4366476]

Bucci C, Parton RG, Mather IH, Stunnenberg H, Simons K, Hoflack B, Zerial M. The small GTPase rab5 functions as a regulatory factor in the early endocytic pathway. Cell. 1992; 70:715–728. [PubMed: 1516130]

Buechner M. Tubes and the single C. elegans excretory cell. Trends Cell Biol. 2002; 12:479–484. [PubMed: 12441252]

Buechner M, Hall DH, Bhatt H, Hedgecock EM. Cystic Canal Mutants in *Caenorhabditis elegans* Are Defective in the Apical Membrane Domain of the Renal (Excretory). Cell. Developmental biology. 1999; 214:227–241.

Chavrier P, Parton RG, Hauri HP, Simons K, Zerial M. Localization of low molecular weight GTP binding proteins to exocytic and endocytic compartments. Cell. 1990; 62:317–329. [PubMed: 2115402]

Chen CC, Schweinsberg PJ, Vashist S, Mareiniss DP, Lambie EJ, Grant BD. RAB-10 is required for endocytic recycling in the Caenorhabditis elegans intestine. Mol Biol Cell. 2006; 17:1286–1297. [PubMed: 16394106]

Chitwood, MB.; Chitwood, BG. The excretory system. In: Chitwood, BG.; Chitwood, MG., editors. Introduction to Nematology. University Park Press; Baltimore, Maryland: 1974. p. 126-135.

Delague V, Jacquier A, Hamadouche T, Poitelon Y, Baudot C, Boccaccio I, Chouery E, Chaouch M, Kassouri N, Jabbour R, Grid D, Megarbane A, Haase G, Levy N. Mutations in FGD4 encoding the Rho GDP/GTP exchange factor FRABIN cause autosomal recessive Charcot-Marie-Tooth type 4H. Am J Hum Genet. 2007; 81:1–16. [PubMed: 17564959]

Egorov MV, Capestrano M, Vorontsova OA, Di Pentima A, Egorova AV, Mariggio S, Ayala MI, Tete S, Gorski JL, Luini A, Buccione R, Polishchuk RS. Faciogenital dysplasia protein (FGD1) regulates export of cargo proteins from the golgi complex via Cdc42 activation. Mol Biol Cell. 2009; 20:2413–2427. [PubMed: 19261807]

Estrada L, Caron E, Gorski JL. Fgd1, the Cdc42 guanine nucleotide exchange factor responsible for faciogenital dysplasia, is localized to the subcortical actin cytoskeleton and Golgi membrane. Hum Mol Genet. 2001; 10:485–495. [PubMed: 11181572]

Fujita M, Hawkinson D, King KV, Hall DH, Sakamoto H, Buechner M. The role of the ELAV homologue EXC-7 in the development of the Caenorhabditis elegans excretory canals. Developmental biology. 2003; 256:290–301. [PubMed: 12679103]

Gao J, Estrada L, Cho S, Ellis RE, Gorski JL. The Caenorhabditis elegans homolog of FGD1, the human Cdc42 GEF gene responsible for faciogenital dysplasia, is critical for excretory cell morphogenesis. Hum Mol Genet. 2001; 10:3049–3062. [PubMed: 11751687]

Gaullier JM, Simonsen A, D'Arrigo A, Bremnes B, Stenmark H, Aasland R. FYVE fingers bind PtdIns(3)P. Nature. 1998; 394:432–433. [PubMed: 9697764]

Gettner SN, Kenyon C, Reichardt LF. Characterization of β*pat-3* heterodimers, a family of essential integrin receptors in *C. elegans*. The Journal of Cell Biology. 1995; 129:1127–1141. [PubMed: 7744961]

Gobel V, Barrett PL, Hall DH, Fleming JT. Lumen morphogenesis in C. elegans requires the membrane-cytoskeleton linker erm-1. Developmental cell. 2004; 6:865–873. [PubMed: 15177034]

Graham TR, Kozlov MM. Interplay of proteins and lipids in generating membrane curvature. Curr Opin Cell Biol. 2010; 22:430–436. [PubMed: 20605711]

Grant BD, Donaldson JG. Pathways and mechanisms of endocytic recycling. Nat Rev Mol Cell Biol. 2009; 10:597–608. [PubMed: 19696797]

Hahn-Windgassen A, Van Gilst MR. The Caenorhabditis elegans HNF4alpha Homolog, NHR-31, mediates excretory tube growth and function through coordinate regulation of the vacuolar ATPase. PLoS Genet. 2009; 5:e1000553. [PubMed: 19668342]

Harris KP, Tepass U. Cdc42 and Par proteins stabilize dynamic adherens junctions in the Drosophila neuroectoderm through regulation of apical endocytosis. J Cell Biol. 2008; 183:1129–1143. [PubMed: 19064670]

Harris KP, Tepass U. Cdc42 and vesicle trafficking in polarized cells. Traffic. 2010

Harris PC, Torres VE. Polycystic Kidney Disease. Annu Rev Med. 2008

Hedgecock EM, Culotti JG, Hall DH, Stern BD. Genetics of cell and axon migrations in Caenorhabditis elegans. Development. 1987; 100:365–382. [PubMed: 3308403]

Hermann GJ, Schroeder LK, Hieb CA, Kershner AM, Rabbitts BM, Fonarev P, Grant BD, Priess JR. Genetic analysis of lysosomal trafficking in Caenorhabditis elegans. Mol Biol Cell. 2005; 16:3273–3288. [PubMed: 15843430]

Hisamoto N, Moriguchi T, Urushiyama S, Mitani S, Shibuya H, Matsumoto K. Caenorhabditis elegans WNK-STE20 pathway regulates tube formation by modulating ClC channel activity. EMBO Rep. 2008; 9:70–75. [PubMed: 18049475]

Huber C, Martensson A, Bokoch GM, Nemazee D, Gavin AL. FGD2, a CDC42-specific exchange factor expressed by antigen-presenting cells, localizes to early endosomes and active membrane ruffles. J Biol Chem. 2008; 283:34002–34012. [PubMed: 18838382]

Kesavan G, Sand FW, Greiner TU, Johansson JK, Kobberup S, Wu X, Brakebusch C, Semb H. Cdc42-mediated tubulogenesis controls cell specification. Cell. 2009; 139:791–801. [PubMed: 19914171]

Kjer-Nielsen L, Teasdale RD, van Vliet C, Gleeson PA. A novel Golgi-localisation domain shared by a class of coiled-coil peripheral membrane proteins. Curr Biol. 1999; 9:385–388. [PubMed: 10209125]

Kumfer KT, Cook SJ, Squirrell JM, Eliceiri KW, Peel N, O'Connell KF, White JG. CGEF-1 and CHIN-1 regulate CDC-42 activity during asymmetric division in the Caenorhabditis elegans embryo. Mol Biol Cell. 2010; 21:266–277. [PubMed: 19923324]

Levi BP, Ghabrial AS, Krasnow MA. Drosophila talin and integrin genes are required for maintenance of tracheal terminal branches and luminal organization. Development. 2006; 133:2383–2393. [PubMed: 16720877]

Liegeois S, Benedetto A, Michaux G, Belliard G, Labouesse M. Genes required for osmoregulation and apical secretion in Caenorhabditis elegans. Genetics. 2007; 175:709–724. [PubMed: 17179093]

Lubarsky B, Krasnow MA. Tube morphogenesis: making and shaping biological tubes. Cell. 2003; 112:19–28. [PubMed: 12526790]

Luschnig S, Batz T, Armbruster K, Krasnow MA. serpentine and vermiform encode matrix proteins with chitin binding and deacetylation domains that limit tracheal tube length in Drosophila. Curr Biol. 2006; 16:186–194. [PubMed: 16431371]

Martin-Belmonte F, Mostov K. Regulation of cell polarity during epithelial morphogenesis. Curr Opin Cell Biol. 2008; 20:227–234. [PubMed: 18282696]

Mattingly, B. Ph.D. Thesis. University of Kansas; 2011. EXC-5 Controls Intracellular Trafficking in Order to Maintain the Structure of the *C. elegans* Excretory Canal.

McCaffrey LM, Macara IG. The Par3/aPKC interaction is essential for end bud remodeling and progenitor differentiation during mammary gland morphogenesis. Genes Dev. 2009; 23:1450–1460. [PubMed: 19528321]

Moore RH, Millman EE, Alpizar-Foster E, Dai W, Knoll BJ. Rab11 regulates the recycling and lysosome targeting of beta2-adrenergic receptors. J Cell Sci. 2004; 117:3107–3117. [PubMed: 15190120]

Mu FT, Callaghan JM, Steele-Mortimer O, Stenmark H, Parton RG, Campbell PL, McCluskey J, Yeo JP, Tock EP, Toh BH. EEA1, an early endosome-associated protein. EEA1 is a conserved alpha-helical peripheral membrane protein flanked by cysteine “fingers” and contains a calmodulin-binding IQ motif. J Biol Chem. 1995; 270:13503–13511. [PubMed: 7768953]

Munro S, Nichols BJ. The GRIP domain - a novel Golgi-targeting domain found in several coiled-coil proteins. Curr Biol. 1999; 9:377–380. [PubMed: 10209120]

Naslavsky N, Caplan S. C-terminal EH-domain-containing proteins: consensus for a role in endocytic trafficking, EH? J Cell Sci. 2005; 118:4093–4101. [PubMed: 16155252]

Nelson FK, Albert PS, Riddle DS. Fine structure of the *Caenorhabditis elegans* secretory-excretory system. Journal of Ultrastructural Research. 1983; 82:156–171.

Nelson FK, Riddle DL. Functional study of the *Caenorhabditis elegans* secretory-excretory system using laser microsurgery. Journal of Experimental Zoology. 1984; 231:45–56. [PubMed: 6470649]

Oka T, Toyomura T, Honjo K, Wada Y, Futai M. Four subunit a isoforms of Caenorhabditis elegans vacuolar H+-ATPase. Cell-specific expression during development. J Biol Chem. 2001; 276:33079–33085. [PubMed: 11441002]

Olson MF, Pasteris NG, Gorski JL, Hall A. Faciogenital dysplasia protein (FGD1) and Vav, two related proteins required for normal embryonic development, are upstream regulators of Rho GTPases. Curr Biol. 1996; 6:1628–1633. [PubMed: 8994827]

Ono Y, Nakanishi H, Nishimura M, Kakizaki M, Takahashi K, Miyahara M, Satoh-Horikawa K, Mandai K, Takai Y. Two actions of frabin: direct activation of Cdc42 and indirect activation of Rac. Oncogene. 2000; 19:3050–3058. [PubMed: 10871857]

Pant S, Sharma M, Patel K, Caplan S, Carr CM, Grant BD. AMPH-1/Amphiphysin/Bin1 functions with RME-1/Ehd1 in endocytic recycling. Nat Cell Biol. 2009; 11:1399–1410. [PubMed: 19915558]

Pasteris NG, Cadle A, Logie LJ, Porteous ME, Schwartz CE, Stevenson RE, Glover TW, Wilroy RS, Gorski JL. Isolation and characterization of the faciogenital dysplasia (Aarskog-Scott syndrome) gene: a putative Rho/Rac guanine nucleotide exchange factor. Cell. 1994; 79:669–678. [PubMed: 7954831]

Praitis V, Casey E, Collar D, Austin J. Creation of low-copy integrated transgenic lines in Caenorhabditis elegans. Genetics. 2001; 157:1217–1226. [PubMed: 11238406]

Praitis V, Ciccone E, Austin J. SMA-1 spectrin has essential roles in epithelial cell sheet morphogenesis in C. elegans. Developmental biology. 2005; 283:157–170. [PubMed: 15890334]

Ren M, Xu G, Zeng J, De Lemos-Chiarandini C, Adesnik M, Sabatini DD. Hydrolysis of GTP on rab11 is required for the direct delivery of transferrin from the pericentriolar recycling compartment to the cell surface but not from sorting endosomes. Proc Natl Acad Sci U S A. 1998; 95:6187–6192. [PubMed: 9600939]

Roberts RC, Peden AA, Buss F, Bright NA, Latouche M, Reilly MM, Kendrick-Jones J, Luzio JP. Mistargeting of SH3TC2 away from the recycling endosome causes Charcot-Marie-Tooth disease type 4C. Hum Mol Genet. 2010; 19:1009–1018. [PubMed: 20028792]

Rodriguez-Fraticelli AE, Vergarajauregui S, Eastburn DJ, Datta A, Alonso MA, Mostov K, Martin-Belmonte F. The Cdc42 GEF Intersectin 2 controls mitotic spindle orientation to form the lumen during epithelial morphogenesis. J Cell Biol. 2010; 189:725–738. [PubMed: 20479469]

Rojas R, Ruiz WG, Leung SM, Jou TS, Apodaca G. Cdc42-dependent modulation of tight junctions and membrane protein traffic in polarized Madin-Darby canine kidney cells. Mol Biol Cell. 2001; 12:2257–2274. [PubMed: 11514615]

Rondanino C, Rojas R, Ruiz WG, Wang E, Hughey RP, Dunn KW, Apodaca G. RhoB-dependent modulation of postendocytic traffic in polarized Madin-Darby canine kidney cells. Traffic. 2007; 8:932–949. [PubMed: 17547697]

Schink KO, Bolker M. Coordination of cytokinesis and cell separation by endosomal targeting of a Cdc42-specific guanine nucleotide exchange factor in Ustilago maydis. Mol Biol Cell. 2009; 20:1081–1088. [PubMed: 19073889]

Senderek J, Bergmann C, Weber S, Ketelsen UP, Schorle H, Rudnik-Schoneborn S, Buttner R, Buchheim E, Zerres K. Mutation of the SBF2 gene, encoding a novel member of the myotubularin family, in Charcot-Marie-Tooth neuropathy type 4B2/11p15. Hum Mol Genet. 2003; 12:349–356. [PubMed: 12554688]

Sharma M, Naslavsky N, Caplan S. A role for EHD4 in the regulation of early endosomal transport. Traffic. 2008; 9:995–1018. [PubMed: 18331452]

Shi A, Pant S, Balklava Z, Chen CC, Figueroa V, Grant BD. A novel requirement for C. elegans Alix/ALX-1 in RME-1-mediated membrane transport. Curr Biol. 2007; 17:1913–1924. [PubMed: 17997305]

Shioi G, Shoji M, Nakamura M, Ishihara T, Katsura I, Fujisawa H, Takagi S. Mutations affecting nerve attachment of Caenorhabditis elegans. Genetics. 2001; 157:1611–1622. [PubMed: 11290717]

Stendel C, Roos A, Deconinck T, Pereira J, Castagner F, Niemann A, Kirschner J, Korinthenberg R, Ketelsen UP, Battaloglu E, Parman Y, Nicholson G, Ouvrier R, Seeger J, De Jonghe P, Weis J, Kruttgen A, Rudnik-Schoneborn S, Bergmann C, Suter U, Zerres K, Timmerman V, Relvas JB, Senderek J. Peripheral nerve demyelination caused by a mutant Rho GTPase guanine nucleotide exchange factor, frabin/FGD4. Am J Hum Genet. 2007; 81:158–164. [PubMed: 17564972]

Stendel C, Roos A, Kleine H, Arnaud E, Ozcelik M, Sidiropoulos PN, Zenker J, Schupfer F, Lehmann U, Sobota RM, Litchfield DW, Luscher B, Chrast R, Suter U, Senderek J. SH3TC2, a protein mutant in Charcot-Marie-Tooth neuropathy, links peripheral nerve myelination to endosomal recycling. Brain. 2010; 133:2462–2474. [PubMed: 20826437]

Stenmark H, Parton RG, Steele-Mortimer O, Lutcke A, Gruenberg J, Zerial M. Inhibition of rab5 GTPase activity stimulates membrane fusion in endocytosis. EMBO J. 1994; 13:1287–1296. [PubMed: 8137813]

Stringham EG, Schmidt KL. Navigating the cell. Cell Adhesion Migration. 2009; 3:342–246. [PubMed: 19684480]

Sulston JE, Schierenberg E, White JG, Thomson JN. The embryonic cell lineage of the nematode Caenorhabditis elegans. Developmental biology. 1983; 100:64–119. [PubMed: 6684600]

Suzuki N, Buechner M, Nishiwaki K, Hall DH, Nakanishi H, Takai Y, Hisamoto N, Matsumoto K. A putative GDP-GTP exchange factor is required for development of the excretory cell in Caenorhabditis elegans. EMBO Rep. 2001; 2:530–535. [PubMed: 11415987]

Teramoto T, Sternick LA, Kage-Nakadai E, Sajjadi S, Siembida J, Mitani S, Iwasaki K, Lambie EJ. Magnesium Excretion in C. elegans Requires the Activity of the GTL-2 TRPM Channel. PLoS One. 2010; 5:e9589. [PubMed: 20221407]

Tong X, Buechner M. CRIP homologues maintain apical cytoskeleton to regulate tubule size in C. elegans. Developmental biology. 2008; 317:225–233. [PubMed: 18384766]

Whitehead IP, Abe K, Gorski JL, Der CJ. CDC42 and FGD1 cause distinct signaling and transforming activities. Mol Cell Biol. 1998; 18:4689–4697. [PubMed: 9671479]

Yandell MD, Edgar LG, Wood WB. Trimethylpsoralen induces small deletion mutations in Caenorhabditis elegans. Proc Natl Acad Sci U S A. 1994; 91:1381–1385. [PubMed: 7906415]

Research Highlights

- Loss of EXC-5 allows narrow tubules to swell into fluid-filled cysts
- Loss of EXC-5 causes accumulation of early endosome marker EEA-1 in cysts
- Sorting endosome marker RME-1 is depleted in cysts
- Buildup of EEA-1 precedes collapse of tubules into cysts
- CDC-42 activity partially rescues loss of EXC-5, phenocopies EXC-5 overexpression

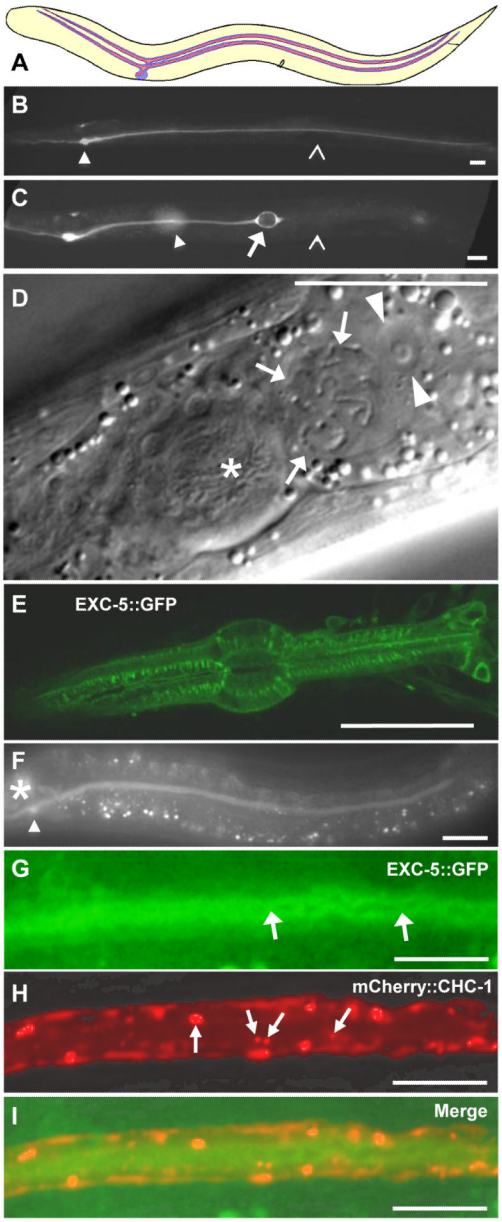


**Fig. 1.**

Varying expression of EXC-5 alters canal morphology. (A) Diagram showing location of the canals within the nematode; anterior left, dorsal top. Apical (luminal) surface in red, basolateral surface in blue, lumen in pink. Excretory canal cell body is located on ventral side midway between the anterior end of the animal and the vulva (black notch) in middle of animal. (B, C) Animals contain the stable integrant *qpIs11*, which strongly expresses GFP beginning in embryogenesis prior to canal extension, driven by the *vha-1* promoter, throughout the cytoplasm of the excretory canal cell and head mesodermal cell (Fujita et al., 2003). (B) Fluorescence micrograph of animal wild-type for *exc-5* shows normal canal morphology. Left-hand anterior and posterior canals are shown (right-hand canal is out of plane of focus) branching from cell body (arrowhead). Open arrowhead marks position of vulva in center of animal. (C) Animal deleted for *exc-5* shows a posterior canal terminating in a large fluid-filled cyst (arrow) anterior to the vulva (open arrowhead). Cyst terminating

the opposing posterior canal is partially visible as a blur at even more anterior position (arrowhead). (D) DIC image of animal overexpressing *exc-5::gfp*. Excretory canal cell body, located just posterior to posterior pharyngeal bulb (asterisk) is filled with convoluted normal-diameter excretory tubule (arrows); nucleus of excretory cell is shown by arrowheads. (E-F) Homozygous expression of low-copy number integrant *qpIs78* (*exc-5::gfp*) in an N2 (wild-type) background (4 copies total of *exc-5*). Panel E shows confocal image showing expression along actin fibers in the pharynx, while panel F shows that expression caused shortening of the canals, but canal extension occurred, and cysts did not form. Asterisk indicates position of posterior pharyngeal bulb, arrowhead is canal cell body. (G-I) Higher magnification of posterior canal expressing integrated low-copy-number constructs of *exc-5::gfp* and membrane-delimited marker *mCherry::chc-1* (clathrin) indicates that EXC-5 is primarily located at the apical (luminal) side of cytoplasm. Most clathrin is located on the basolateral side of the canal, but some is more apical (arrows in H), possibly connected to the tubulovesicular canaliculi where EXC-5 appears concentrated: (G) EXC-5, green; (H) CHC-1, red; (G) superimposed. Anterior is to the left in all figures, ventral to the bottom in all panels except D. All animals are either L4s or young adults. All fluorescence panels brightened and contrast-enhanced to show location of highest concentrations of weak GFP fluorescence. Bars, 100 μm in panels B and C, 50 μm in all others.

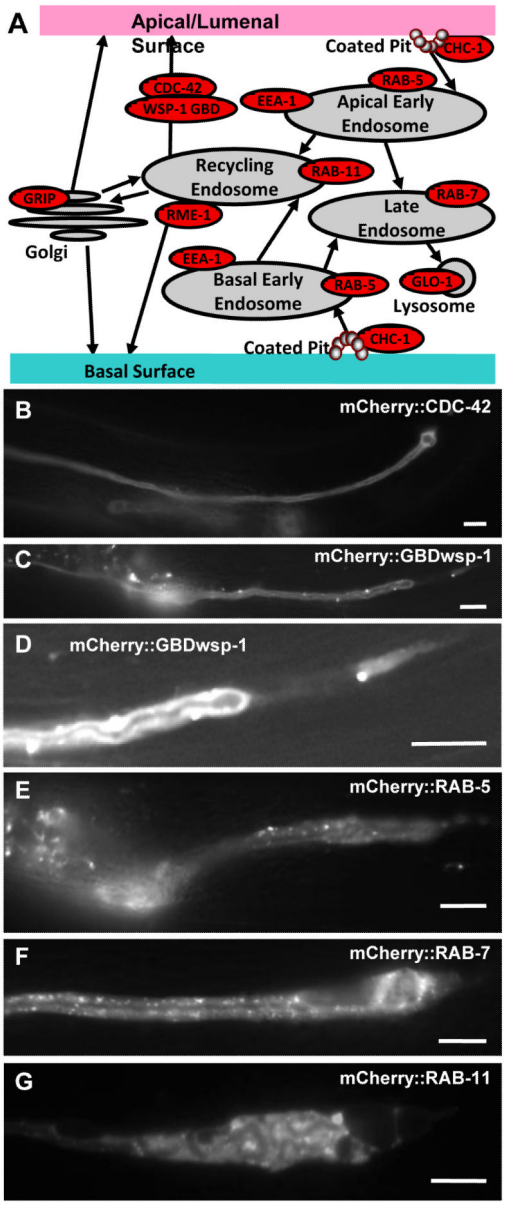


**Fig. 2.**

Expression of some subcellular markers within the excretory canals occasionally altered canal morphology. (A) Model of vesicular transport in the excretory canals, with markers used in this study to indicate various subcellular compartments. (B-G) Fluorescence micrographs of typical segments of posterior canal in young adult animals. All markers were expressed in constructs linked to mCherry and driven by the *exc-9* promoter. (B) Small GTPase CDC-42. (C) The domain of WSP-1 that binds to activated (GTP-bound) CDC-42. (D) Enlarged and brightened area of Fig. 2C at distal tip of GBDwsp-1-labeled canal shows "tail" of cytoplasm disconnected from lumen. (E) RAB-5; (F) RAB-7; (G) RAB-11. Bars, 50 μm. Micrographs were taken with Optronics camera either in black/white or RGB color mode, and are not altered, except for contrast enhancement of Fig. 2D and converting Fig. 2G from color to b/w.

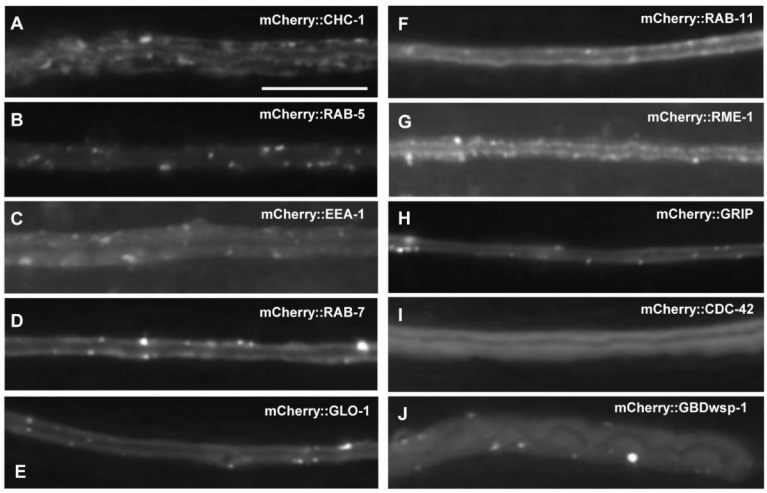


**Fig. 3.**

Expression of subcellular markers within the excretory canals in wild-type animals. Fluorescence micrographs of typical segments of posterior canal in young adult animals. All markers were expressed from constructs linked to mCherry and driven by the *exc-9* promoter. Bar, 50 μm. (A) CHC-1; (B) RAB-5; (C) EEA-1; (D) RAB-7; (E) GLO-1; (F) RAB-11; (G) RME-1; (H) GRIP; (I) CDC-42; (J) WSP-1 GTP-binding domain.

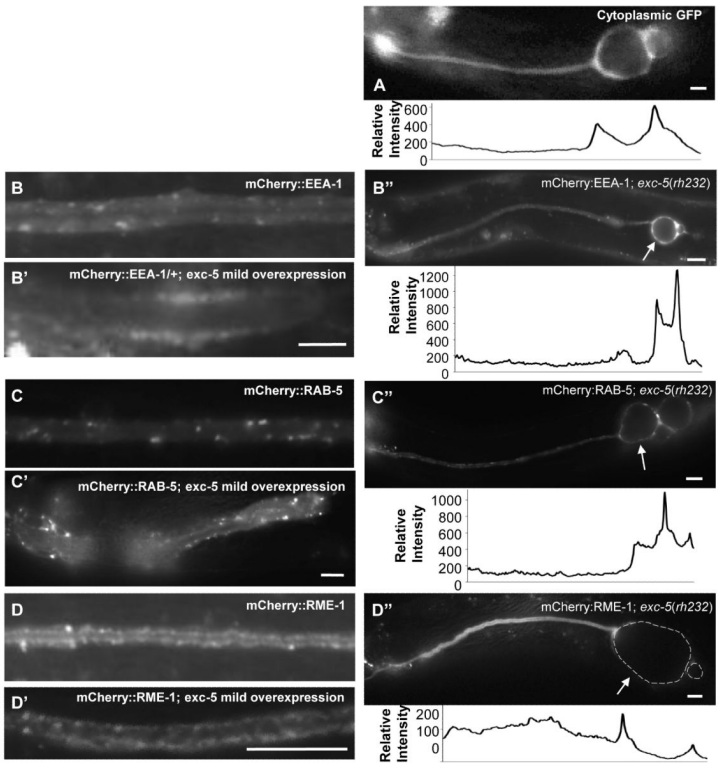


**Fig. 4.**

Effect of variation of EXC-5 level on subcellular marker distribution. Young adult animals of *exc-5*(*rh232*) expressing integrated constructs containing subcellular markers. Relative brightness along the length of the canals is shown beneath each panel of animals deleted for *exc-5*, normalized to normal-diameter canal brightness. (A) Animal exhibits cytoplasmic GFP driven by the strong canal-specific *vha-1* promoter. (B-D) Animals express subcellular markers linked to mCherry, and driven by the *exc-9* promoter; stronger expression of these markers altered canal morphology. (B,C,D) Controls: Markers in animals containing wild-type levels of EXC-5 (from panels C, B, and G of Fig. 3); (B', C', D') markers in animals with overexpression of *exc-5*; (B", C", D") markers in animals lacking EXC-5. (B-B") EEA-1. In *exc-5* mutant, the highest levels of fluorescence surround area of fluid-filled cysts at canal terminus (arrow). (C-C") RAB-5. In *exc-5* mutants, this marker shows higher amounts of fluorescence surrounding the cyst than in normal-diameter tubule. (D-D") RME-1. In *exc-5* mutant panel (D"), the dashed grey circles outline lumen of large fluid-filled cysts (arrow) at canal terminus. Bars, 50 μm.

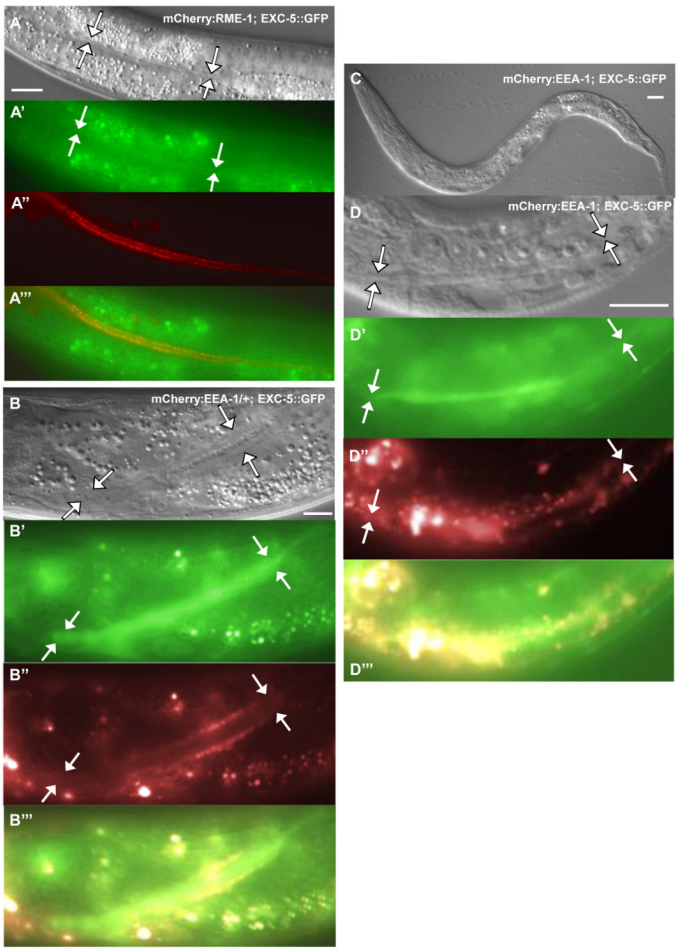


**Fig. 5.**

EXC-5 overexpression alters subcellular marker distribution. Excretory canal cells of young adult animals containing integrated homozygous *exc-5*::*gfp* constructs (presumably 4 copies total of *exc-5*), in addition to integrated constructs of subcellular markers linked to mCherry driven by the *exc-9* promoter. (A-A'") RME-1; (B-B'") Dying L1 larva homozygous both for *mCherry*::*eea-1* and for *exc-5*::*gfp* (in a background wild-type for *exc-5*, or presumably 4 doses of *exc-5* total); (C, D-D'") Young adult animal heterozygous for *mCherry*::*eea-1* and homozygous for *exc-5*::*gfp* (in a background wild-type for *exc-5*, or presumably 4 doses of *exc-5* total). Panels A, B, C, D: DIC images. Panels A', B', D', expression of EXC-5::GFP; images contrast-enhanced to emphasize position of very weakly fluorescent GFP (especially in Fig. 5b, in which level of GFP fluorescence was very low). Arrows indicate position of canal. Panels A", B", D", markers linked to mCherry. Panels A'", B'", D'", green/red merge. Bars, 50 μm.

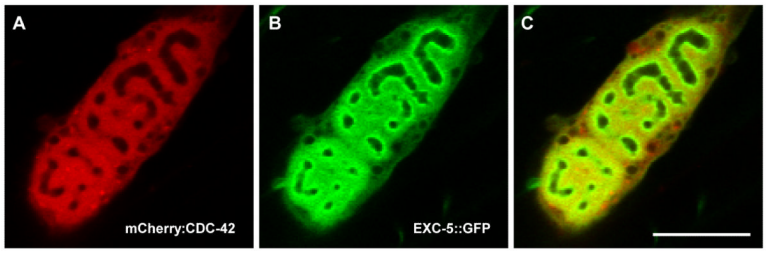


**Fig. 6.**

Confocal images of subcellular location of EXC-5 and activated CDC-42 in convoluted excretory canal tubule of animal expressing both homozygous *mCherry::cdc-42* and functional *exc-5::gfp* constructs. (A) mCherry::CDC-42 is concentrated around the convoluted tubular area, with some elevated levels of fluorescence also evident throughout the rest of the cell. (B) EXC-5::GFP is strongly concentrated in the subapical region surrounding the convoluted excretory canal tubule and canaliculi. (C) Merged micrographs. All photographs false-colored and contrast-enhanced to highlight areas of highest fluorescence. Bar, 50 μm.

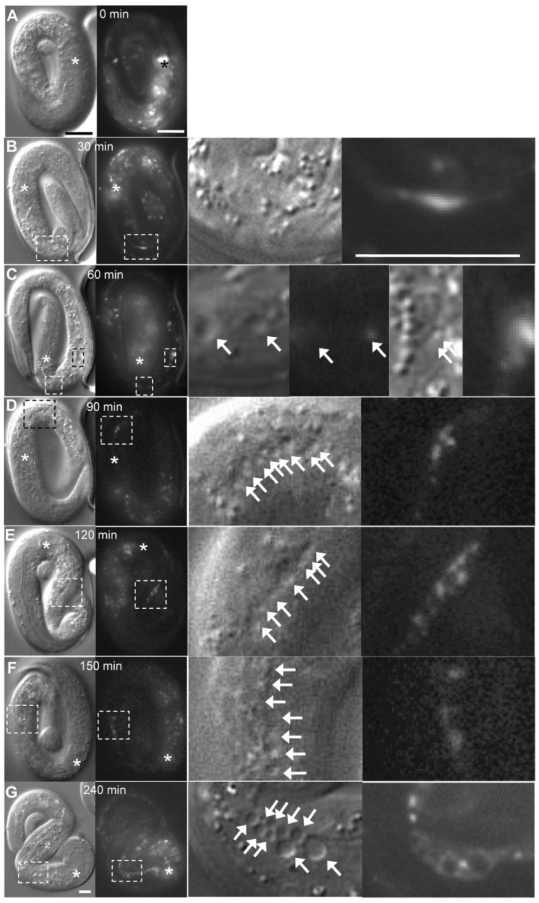


**Fig. 7.**

Alteration of subcellular marker expression precedes cyst formation in *exc-5*(*rh232*) animal. (A-G) DIC and fluorescence micrographs of a single animal expressing *mCherry*::*eea-1* driven by the *exc-9* promoter, beginning at the 3-fold stage of embryogenesis. The fluorescent marker is evident in many head neurons at this stage as well as in the excretory canal cell. Images were taken at the times indicated, starting at the point at which observation of the animal began. Wild-type embryos hatch within 2 hours of the 3-fold stage at 20°C (Sulston et al., 1983). Cysts appear in DIC micrographs with DIC “shadow” to the upper left of the cyst. Gut granules and other subcellular organelles show a DIC “shadow” to the lower right of the object. Animal was moving inside the embryo; DIC and fluorescence micrographs show similar positions, but cannot always be directly overlaid. Boxed areas indicate the same areas of the animal, and are enlarged in panels to the right. An asterisk designates the posterior pharyngeal bulb. Arrows in enlarged DIC micrographs show cysts. (A) No cysts were evident in the canals, and *eea-1* fluorescence was barely detectable in the left-hand posterior canal. (B) Localized *eea-1* accumulation is evident in the canal, while no cysts have formed. (C) The area exhibiting *eea-1* fluorescence in panel (B) now shows small cysts (right-hand enlarged panels), while *eea-1* fluorescence is now evident in a new area near the cell body (left-hand enlarged panels). (D-F) accumulation of marked *eea-1* persists throughout this area of the posterior canal as cysts become evident. (G) By the time of hatching, the area of *eea-1* accumulation has spread and intensified, many new cysts have formed, and cysts have greatly enlarged. Brightness and contrast was enhanced in DIC micrographs only to show cysts more clearly. Fluorescence micrographs were brightened

and contrast increased to show areas of greatest canal fluorescence. In enlarged panels, DIC micrographs only were digitally sharpened. Bars, 50 μm.

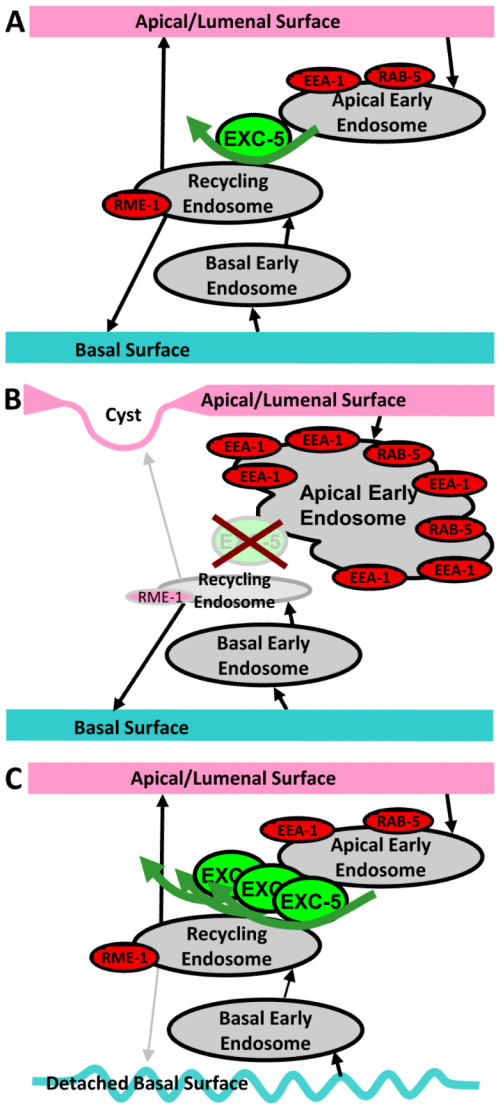


**Fig. 8.**

Model for effects of EXC-5 on organelle movement. (A) EXC-5 mediates the passage of early endosomes to recycling endosomes, presumably through activation of CDC-42 as well as other small GTPases. (B) Loss of EXC-5 through mutation prevents movement of apical early endosomes, marked by RAB-5 and especially by EEA-1, which then accumulate. As less movement of early endosomes is inhibited, the appearance of the recycling endosome marker RME-1 is depleted. Loss of membrane-bound proteins at the apical surface cause weakening of this surface, eventually to break under osmotic pressure from the canal lumen, to form a fluid-filled cyst. (C) Overexpression of EXC-5 enhances apical recycling, so that the apical surface is maintained and lumen diameter remains narrow. The large amount of apical endosomes presumably passing through the recycling endosome prevents efficient passage of material from the basal early endosome, presumably including membrane proteins such as integrins that bind to the basement membrane. Slow recycling of these proteins to the basal surface allows delamination of these cells from their basement membranes, as seen in animals overexpressing *exc-5* (Suzuki et al., 2001), and extension of the canals is halted.

## Table 1

### Strains used for this study

| Strain | Genotype | Description | Reference |
|---|---|---|---|
| N2 | | wild-type | (Brenner, 1974) |
| NJ731 | *exc-5(rh232)* | *exc-5* deletion | (Suzuki et al., 2001) |
| BK36 | unc-*119(ed3); qpIs11[unc-119; Pvha-1::gfp]* I | wild-type with integrated GFP marker expressed in excretory canals | This study |
| BK30 | *exc-5(rh232); qpIs11[unc-119; Pvha-1::gfp]* I | NJ731 crossed to BK36 to express integrated GFP marker in an exc-5 mutant background | This study |
| BK179 | N2; *qpIs78[exc-5::gfp*; N2 DNA] X | integrated low-copy-number EXC-5::GFP fusion | This study |
| Wild-type strains expressing mCherry-labeled marker genes | | **mCherry Marker labels:** | |
| BK219 | N2; *qpIs102[Pexc-9::mCherry::chc-1]* | CHC-1: clathrin-coated pits | This study |
| BK201 | N2; *qpIs95[Pexc-9::mCherry::eea-1]* X | EEA-1: early endosomes | This study |
| BK209 | N2; *qpIs99[Pexc-9::mCherry::rab-5]* IV | RAB-5: early endosomes | This study |
| BK210 | N2; *qpIs100[Pexc-9::mCherry::rab-7]* | RAB-7: late endosomes | This study |
| BK206 | N2; *qpIs98[Pexc-9::mCherry::glo-1]* | GLO-1: lysosomes | This study |
| BK211 | N2; *qpIs101[Pexc-9::mCherry::rme-1]* X | RME-1: recycling endosomes | This study |
| BK205 | N2; *qpIs97[Pexc-9::mCherry::rab-11]* V | RAB-11: recycling endosomes | This study |
| BK220 | N2; *qpIs103[Pexc-9::mCherry::GRIP]* | GRIP: Golgi apparatus | This study |
| BK204 | N2; *qpIs96[Pexc-9::mCherry::cdc-42]* | CDC-42: cytoplasm | This study |
| BK262 | N2; *qpIs104[Pexc-9::mCherry::GBDwsp-1]* | GBD domain of WSP-1: cytoplasm | This study |
| *exc-5* deletion strains with mCherry-labeled markers | | | |
| BK221 | NJ731; *qpIs102[Pexc-9::mCherry::chc-1]* | CHC-1: clathrin-coated pits | This study |
| BK218 | NJ731; *qpIs95[Pexc-9::mCherry::eea-1]* X | EEA-1: early endosomes | This study |
| BK217 | NJ731; *qpIs99[Pexc-9::mCherry::rab-5]* IV | RAB-5: early endosomes | This study |
| BK216 | NJ731; *qpIs100[Pexc-9::mCherry::rab-7]* | RAB-7: late endosomes | This study |
| BK213 | NJ731; *qpIs98[Pexc-9::mCherry::glo-1]* | GLO-1: lysosomes | This study |
| BK214 | NJ731; *qpIs101[Pexc-9::mCherry::rme-1]* X | RME-1: recycling endosomes | This study |
| BK215 | NJ731; *qpIs97[Pexc-9::mCherry::rab-11]* V | RAB-11: recycling endosomes | This study |
| BK222 | NJ731; *qpIs103[Pexc-9::mCherry::GRIP]* | GRIP: Golgi apparatus | This study |
| BK212 | NJ731; *qpIs96[Pexc-9::mCherry::cdc-42]* | CDC-42: cytoplasm | This study |
| BK273 | NJ731; *qpIs104[Pexc-9::mCherry::GBDwsp-1]* | GBD domain of WSP-1: cytoplasm | This study |
| Strains with slight overexpression of exc-5 (labeled with GFP) containing mCherry-labeled markers | | | |
| BK227 | BK179; *qpIs102[Pexc-9::mCherry::chc-1]* | CHC-1: clathrin-coated pits | This study |
| BK230 | BK179; *qpIs95[Pexc-9::mCherry::eea-1]* X | EEA-1: early endosomes | This study |
| BK226 | BK179; *qpIs99[Pexc-9::mCherry::rab-5]* IV | RAB-5: early endosomes | This study |
| BK224 | BK179; *qpIs100[Pexc-9::mCherry::rab-7]* | RAB-7: late endosomes | This study |
| BK228 | BK179; *qpIs98[Pexc-9::mCherry::glo-1]* | GLO-1: lysosomes | This study |
| BK223 | BK179; *qpIs101[Pexc-9::mCherry::rme-1]* X | RME-1: recycling endosomes | This study |
| BK225 | BK179; *qpIs97[Pexc-9::mCherry::rab-11]* V | RAB-11: recycling endosomes | This study |
| BK229 | BK179; *qpIs103[Pexc-9::mCherry::GRIP]* | GRIP: Golgi apparatus | This study |

| Strain | Genotype | Description | Reference |
|---|---|---|---|
| BK231 | BK179; *qpIs96[Pexc-9::mCherry::cdc-42]* | CDC-42: cytoplasm | This study |
| BK274 | BK179; *qpIs104[Pexc-9::mCherry::GBDwsp-1]* | GBD domain of WSP-1: cytoplasm | This study |

**Table 2**

**Effects of marker expression on excretory canal phenotype**[a]

| Strain/Genotype | n[b] | Convoluted[c] | Canal Length[d] | Cystic[e] | # Cysts[f] | Size of Cysts[g] | | |
|---|---|---|---|---|---|---|---|---|
| | | | | | | Small | Medium | Large |
| N2 (Wild-type) animals: | 100 | 0 | 4.0 | 0 | | | | |
| expressing: *mCherry*::*cdc-42* | 92 | 0 | 3.2 | **20.7** | **0.4** | **2.0** | 0 | 0 |
| *mCherry* :: *wsp-1GBD* | 100 | 7.0 | 1.4 | **2.0** | 0 | **1.0** | **1.0** | **1.0** |
| *mCherry* :: *chc-1* | 100 | 0 | 4.0 | 0 | | | | |
| *mCherry* :: *eea-1* | 99 | 0 | 3.3 | 0 | | | | |
| *mCherry* :: *glo-1* | 100 | 0 | 4.0 | 0 | | | | |
| *mCherry* :: *GRIP* | 100 | 0 | 3.4 | 0 | | | | |
| *mCherry:rab-5* | 100 | 9.0 | 2.9 | 0 | | | | |
| *mCherry* :: *rab-7* | 100 | 0 | 2.5 | 0 | | | | |
| *mCherry* :: *rab-11* | 100 | 7.0 | 3.0 | **2.0** | **0.1** | **2.5** | 0 | 0 |
| *mCherry* :: *rme-1* | 100 | 0 | 3.8 | 0 | | | | |
| trans. express: *gfp*::CA *cdc-42* | 84 | 83.3 | 2.7 | **1.2** | 0 | 1.0 | 0 | 0 |
| *gfp*::DN *cdc-42* | 48 | 0 | 3.1 | **56.3** | **2.8** | **2.6** | **0.2** | 0 |
| NJ731 *exc-5 (rh232)* mutants | 96 | 0 | 1.2 | 100 | 8.6 | 7.5 | 1.7 | 1.1 |
| expressing: *mCherry*::*cdc-42* | 100 | 0 | 1.3 | 100 | 9.8 | 6.9 | 2.3 | 2.0 |
| *mCherry* :: *wsp-1GBD* | 104 | 20.2 | 0.5 | 50.0 | 1.8 | 3.8 | 1.1 | 1.0 |
| *mCherry* :: *chc-1* | 92 | 0 | 1.4 | 98.9 | 6.4 | 4.4 | 2.2 | 1.2 |
| *mCherry* :: *eea-1* | 100 | 0 | 1.6 | 97 | 5.6 | 4.4 | 2.0 | 1.3 |
| *mCherry* :: *glo-1* | 100 | 0 | 1.3 | 98 | 7.8 | 6.0 | 2.2 | 1.2 |
| *mCherry* :: *GRIP* | 100 | 0 | 1.1 | 98 | 8.7 | 6.6 | 2.4 | 1.3 |
| *mCherry:rab-5* | 99 | 0 | 1.1 | 100 | 9.0 | 7.6 | 1.9 | 1.3 |
| *mCherry* :: *rab-7* | 100 | 0 | 1.2 | 100 | **12.0** | **10.0** | 2.5 | 1.4 |
| *mCherry* :: *rab-11* | 100 | 0 | 1.3 | 99 | 8.3 | 7.3 | 1.9 | 1.2 |
| *mCherry* :: *rme-1* | 99 | 0 | 1.3 | 89.9 | 3.8 | 3.4 | 1.8 | 1.4 |
| trans. express: *gfp*::CA *cdc-42* | 54 | 81.5 | 1.6 | 100 | 8.0 | 6.7 | 1.0 | 0.3 |

| Strain/Genotype | n[b] | Convoluted[c] | Canal Length[d] | Cystic[e] | # Cysts[f] | Size of Cysts[g] | | |
|---|---|---|---|---|---|---|---|---|
| | | | | | | Small | Medium | Large |
| *gfp*::DN *cdc-42* | 42 | 0 | 1.6 | 100 | 11.7 | 9.7 | 1.5 | 0.5 |
| BK179 Low *exc-5* overexpress | 100 | 8.0 | 1.5 | 0.0 | | | | |
| expressing: *mCherry*::*cdc-42* | 100 | 84.0 | 0.5 | **5.0** | **0.2** | **3.7** | **1.0** | **1.0** |
| *mCherry* :: *wsp-1GBD* | 102 | 14.7 | 1.1 | 0.0 | | | | |
| *mCherry* :: *chc-1* | 100 | | 2.6 | **1.0** | 0 | **3.0** | 0.0 | 0.0 |
| *mCherry* :: *eea-1* | 74 | | 0.6 | 0.0 | | | | |
| *mCherry* :: *glo-1* | 100 | | 1.3 | 0.0 | | | | |
| *mCherry* :: *GRIP* | 102 | | 1.8 | 0.0 | | | | |
| *mCherry* :: *rab-5* | 99 | 13.1 | 1.1 | **2.0** | 0 | **2.0** | 0.0 | 0.0 |
| *mCherry* :: *rab-7* | 99 | 37.4 | 0.9 | 0.0 | | | | |
| *mCherry* :: *rab-11* | 103 | 68.8 | 0.6 | 0.0 | | | | |
| *mCherry* :: *rme-1* | 100 | | 2.1 | 0.0 | | | | |

[a] Substantial increases in cyst number or size from those of controls without mCherry constructs are indicated in boldface. Increases in number of convoluted tubules and decreases in number of cysts are underlined.

[b] Number of canals examined.

[c] Percentage of canals that exhibited a lumen that traversed itself more than once.

[d] Average canal length relative to body length as described in Materials & Methods; 0 means no canal growth, 4 is full-length.

[e] Percentage of canals that exhibited any visible cysts at all.

[f] Average number of cysts observed for all animals

[g] Average number of large, medium, and small cysts (size determined as described in Materials & Methods) seen for animals exhibiting cysts.

## Table 3
## Effects of loss of EXC-5 on marker expression

| Strain/Genotype | N[a] | % of animals with cysts noticeably brighter than in normal tubule[b] | % of animals with cysts noticeably fainter than in normal tubule |
|---|---|---|---|
| *exc-5* mutants expressing: cytoplasmic GFP ($P_{vha-1}$::*gfp*) | 250 | 28 | 0 |
| *mCherry* :: *cdc-42* | 135 | 34 | 0 |
| *mCherry* :: *GBDwsp-1* | 80 | 24 | 0 |
| *mCherry* :: *chc-1* | 90 | 17 | 4 |
| *mCherry* :: *eea-1* | 207 | 58 | 0 |
| *mCherry* :: *glo-1* | 100 | 26 | 0 |
| *mCherry* :: *GRIP* | 100 | 28 | 0 |
| *mCherry:rab-5* | 100 | 24 | 0 |
| *mCherry* :: *rab-7* | 100 | 23 | 0 |
| *mCherry* :: *rab-11* | 135 | 30 | 0 |
| *mCherry* :: *rme-1* | 100 | 0 | 31 |

[a] Number of canals examined.

[b] Number of animals graded as “bright” was normalized to account for variations in brightness between wild-type animals viewed in different counting sessions.